PHYSICAL REVIEW D VOLUME 21, NUMBER 2 15 JANUARY 1980

Killing horizons and dragging of the inertial frame about a uniformly accelerating particle

Hamid Farhoosh and Robert L. Zimmerman
Department of Physics and Institute of Theoretical Science, University of Oregon, Eugene, Oregon 97403
(Received 3 July 1979)

The structure of Killing horizons in the static vacuum C metric which represents the gravitational field of a uniformly accelerating Schwarzschild-type particle is studied. It is shown that for $A^2m^2 < 1/27$ there exist two physically meaningful horizons. One horizon is analogous to the Schwarzschild surface and the other is similar to a flat surface in Euclidean space traveling at the speed of light along the axis of symmetry. This second surface is called the Rindler surface because of its analogy with the Rindler surface in the limit that geometry becomes Euclidean. As the acceleration increases, the Schwarzschild surface distorts from its original spherical shape. Its shape becomes teardroplike with the pointed end oriented in the direction of the acceleration. In the forward direction the Schwarzschild surface moves outward from the origin as the acceleration continues to increase in accordance with the principle of equivalence. In the backward direction the surface shrinks from its original Schwarzschild surface as the acceleration increases for relatively small values of the acceleration. This is also expected from the principle of equivalence. As the acceleration reaches $A = 1/\sqrt{54}m$ the Schwarzschild surface in the backward direction reaches a minimum distance from the origin at $r = \sqrt{3}m$ and as the acceleration further increases it reverses its direction of motion and grows outward until it reaches the original Schwarzschild surface at $r = 2m$. This behavior is an apparent violation of the principle of equivalence. As the acceleration increases, the Rindler surface moves inward approaching the Schwarzschild surface, and finally when $A = 1/\sqrt{27}m$ the two surfaces unite and produce a naked singularity. Radial geodesic and nongeodesic motions are also investigated. It is shown that for small accelerations the results are in agreement with the principle of equivalence and the effects of dragging of the inertial frame due to the rectilinear acceleration.

I. INTRODUCTION

There are numerous exact solutions of the Einstein field equations. Most of these solutions are solvable because of assumptions of mathematical simplicity and do not correspond to physically interesting cases. Other solutions are so complicated that their properties are of little use. The two most important solutions of the vacuum field equations are the Schwarzschild and Kerr solutions. The Schwarzschild solution has revealed the surface of infinite red-shift and one-way membrane that surrounds a spherically symmetric object. The Kerr solution has generalized these results to allow for uniform rotation and has revealed the existence of the ergosphere and the dragging of the inertial frame. Possibly the third most important vacuum solution is that of a uniformly accelerating particle. This solution will allow us to study the modification of the Schwarzschild surface, the possible dragging of the inertial frame, and the role of the principle of equivalence for an exact solution with uniform rectilinear acceleration.

The vacuum C metric, representing the gravitational field of a uniformly accelerating Schwarzschild-type particle, is a degenerate Weyl vacuum solution. The vacuum C metric was first discovered in 1918 by Levi-Civita.[1] It was rediscovered in 1961 by Newman and Tamburino,[2] and its geometric properties were investigated by Robinson and Trautman in 1962,[3] Ehlers and Kundt in 1963,[4] and Kinnersley and Walker in 1970.[5] Its physical interpretation was first noticed by Kinnersley and Walker[5] and explored further by Plebanski and Demianski[6] and by Ernst.[7] The radiative properties were first studied by Kinnersley and Walker[5] and explored further by Farhoosh and Zimmerman.[8] The mathematical properties of its horizons, Killing tensors, and analytic extension have been investigated by Godfrey,[9,10] Carter,[11] and Hughston[12] and by Kinnersley and Walker.[5] In the present paper we will extend these investigations of the Killing surfaces. We will explore their shape as expressed in a uniformly accelerating coordinate system as well as a nonaccelerating coordinate system. We will also explore the role of the principle of equivalence and the effect of the dragging of the inertial frame by the rectilinear acceleration.

In Sec. II we will present the various different forms of the metric and a physical interpretation of the accelerating and nonaccelerating coordinate systems. In Sec. III the structure of Killing horizons is studied. It is shown in this section that for $A^2m^2 < \frac{1}{27}$, where m is the mass and A is the acceleration of the particle, there are two distinct and physically meaningful Killing horizons. One horizon is similar to the Schwarzschild sur-

face, being caused mainly by the mass of the particle and distorted by the acceleration. The acceleration causes this surface to become elongated in the forward direction, which is the direction towards which the particle is accelerating, and to shrink in the backward direction. The second horizon is governed mainly by the acceleration of the particle and is similar to the Rindler horizon that appears in accelerating coordinate systems.[13] This surface is distorted by the presence of the mass.

The Rindler-type surface surrounds the Schwarzschild-type surface and is open in the forward direction. By increasing the acceleration Schwarzschild-type surface becomes more deformed, expanding in the forward direction and shrinking in the backward direction in accordance with the principle of equivalence. As the acceleration reaches $A = 1/\sqrt{54}m$ the Schwarzschild-type surface in the backward direction reaches a minimum distance from the origin at $r = \sqrt{3}m$, and as the acceleration increases further the surface reverses its direction of motion and grows outward until it reaches the original Schwarzschild surface at $r = 2m$. This behavior is an apparent violation of the principle of equivalence. On the other hand, the Rindler-type surface moves inward as the acceleration increases approaching the Schwarzschild-type surface and at $A = 1/\sqrt{27}m$ the two surfaces unite and form a naked singularity at the origin.

In Secs. IV and V radial geodesic and nongeodesic motions are investigated. The behavior of geodesic motion for small accelerations is shown to be a consequence of the principle of equivalence and the dragging of the inertial frame. These results are summarized in Sec. VI.

II. COORDINATE SYSTEMS

The lack of understanding coordinates often hides the physical interpretation and the properties of many solutions in general relativity. The vacuum C metric is no exception. While some coordinates are more useful for understanding the geometrical properties of the space, others are more convenient for understanding the physical properties of the source and gravitational field. The form of the metric where the mathematical properties of the vacuum C metric are the simplest is[5]

$$ds^2 = \frac{1}{A^2(p+q)^2}(F dt^2 - F^{-1}dq^2 - G^{-1}dp^2 - G d\omega^2), \tag{2.1}$$

where

$$G = G(p) = 1 - p^2 - 2Amp^3, \tag{2.2a}$$

$$F = F(q) = -1 + q^2 - 2Amq^3, \tag{2.2b}$$

m is the mass, and A is the acceleration of the particle. The range of the timelike coordinate t is from $-\infty$ to $+\infty$, while the range of the coordinate ω is from 0 to 2π. The range of the coordinates p and q are determined from the fact that both $G(p)$ and $F(q)$ must remain positive in order to keep the signature of the metric unchanged. We are interested in the case where the values of A are such that $A^2m^2 \leq \frac{1}{27}$. For this range of A the function $G(p)$ has three real roots given by[14]

$$p_\pi = -\frac{1}{6Am}\left[2\cos\left(\frac{\lambda}{3} + \frac{2\pi}{3}\right) + 1\right], \tag{2.3a}$$

$$p_0 = -\frac{1}{6Am}\left[2\cos\left(\frac{\lambda}{3} + \frac{4\pi}{3}\right) + 1\right], \tag{2.3b}$$

$$p_u = -\frac{1}{6Am}\left(2\cos\frac{\lambda}{3} + 1\right), \tag{2.3c}$$

where

$$\cos\lambda = 1 - 54A^2m^2. \tag{2.4}$$

Likewise, the three real roots of the function $F(q)$ are at

$$q_S = -\frac{1}{6Am}\left[2\cos\left(\frac{\delta}{3} + \frac{2\pi}{3}\right) - 1\right], \tag{2.5a}$$

$$q_R = -\frac{1}{6Am}\left[2\cos\left(\frac{\delta}{3} + \frac{4\pi}{3}\right) - 1\right], \tag{2.5b}$$

$$q_u = -\frac{1}{6Am}\left(2\cos\frac{\delta}{3} - 1\right), \tag{2.5c}$$

where

$$\cos\delta = -(1 - 54A^2m^2). \tag{2.6}$$

The functions $G(p)$ and $F(q)$ are plotted in Fig.

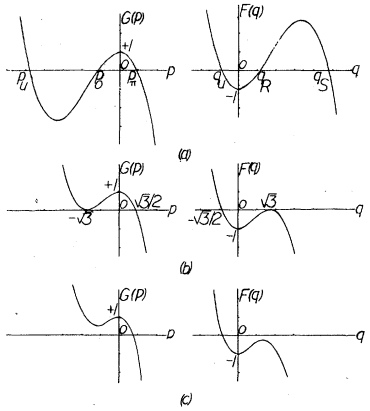

FIG. 1. Cubic functions $G(p)$ and $F(q)$ are plotted for (a) $A < 1/\sqrt{27}m$, (b) $A = 1/\sqrt{27}m$, and (c) $A > 1/\sqrt{27}m$.

1 for different values of A. We see that several different ranges of q and p can be chosen so that $F(q)$ and $G(p)$ are positive. Each one of these choices corresponds to different vacuum solutions. We are interested in the case where the range of p and q are given by

$$q_S \geq q \geq q_R\,, \tag{2.7a}$$

$$p_\pi \geq p \geq p_0\,. \tag{2.7b}$$

We would now like to express Eq. (2.1) in a more physically meaningful coordinate system. Equation (2.1) can be transformed to a uniformly accelerating, null, spherical-like coordinate system by letting

$$r = \frac{1}{A(p+q)} \tag{2.8a}$$

and

$$t = Au + \int_q \frac{dq}{F(q)}\,. \tag{2.8b}$$

The line element (2.1) then transforms to

$$ds^2 = Hdu^2 + 2dudr + 2Ar^2 dudp - r^2(G^{-1}dp^2 + Gd\omega^2)\,, \tag{2.9}$$

where

$$\begin{aligned} H &= A^2r^2F = -A^2r^2G(p - A^{-1}r^{-1}) \\ &= 1 - 2Arp - A^2r^2(1-p^2) - \frac{2m}{r}(1-Arp)^3 \\ &= 1 - \frac{2m}{r} + 6Amp + ArG_{,p} - A^2r^2G(p) \end{aligned} \tag{2.10}$$

and the comma represents the ordinary derivative. The range of the coordinate u is from $-\infty$ to $+\infty$ and the range of the coordinate r is restricted to the region between the points where H is positive.

For the metric in (2.9) the null tetrads are[5,8]

$$\begin{aligned} l^\mu &= (0, 1, 0, 0)\,, \\ n^\mu &= (1, -\tfrac{1}{2}H, 0, 0)\,, \\ m^\mu &= \left(0, -\frac{1}{\sqrt{2}}Ar\sqrt{G(p)}\,, \frac{1}{2}\frac{\sqrt{G(p)}}{r}\,, \frac{i}{\sqrt{2}}\frac{1}{r\sqrt{G(p)}}\right), \end{aligned} \tag{2.11}$$

and the only nonvanishing tetrad component of the curvature tensor is

$$\psi_2 = -\frac{m}{r^3}\,. \tag{2.12}$$

The real singularity $r=0$ in (2.12) is a manifestation of the presence of the Schwarzschild-type particle centered at $r=0$. The line element (2.9) is a degenerate vacuum Weyl solution and has two hypersurface orthogonal Killing vectors given by

$$\xi^\mu_{(t)} = (1, 0, 0, 0)\,, \tag{2.13a}$$

$$\xi^\mu_{(\omega)} = (0, 0, 0, 1)\,, \tag{2.13b}$$

whose norms are

$$\xi^\mu_{(t)}\xi_{(t)\mu} = H = A^2r^2F\,, \tag{2.14a}$$

$$\xi^\mu_{(\omega)}\xi_{(\omega)\mu} = -r^2G(p)\,. \tag{2.14b}$$

μ runs from 0 to 3 denoting u, r, p, ω, respectively. $\xi^\mu_{(t)}$ is the timelike Killing vector representing the time symmetry and the static structure of the metric. $\xi^\mu_{(\omega)}$ being spacelike denotes the axial symmetry of the solution.

In order to interpret the meaning of these coordinates we notice that in the limit $A \to 0$ the line element (2.9) reduces to Schwarzschild line element written in the null coordinates provided that

$$\omega = \varphi \tag{2.15}$$

and

$$G(p, A=0) = 1 - p^2 = \sin^2\theta\,. \tag{2.16}$$

θ and φ are the usual spherical polar and azimuthal angles having the usual range of 0 to π and 0 to 2π, respectively. u is the retarded time and r is the radial coordinate ranging from $2m$ to ∞. In this limit the norm of the spacelike Killing vector $\xi^\mu_{(\omega)}$ in (2.14b) becomes

$$\xi^\mu_{(\omega)}\xi_{(\omega)\mu} = -r^2\sin^2\theta\,. \tag{2.17}$$

To identify the angular coordinate for the case where $A \neq 0$ we retain the relation in (2.15) between the ω and the φ coordinates. To identify the polar angle θ with the p coordinate we require the norm of the axial Killing vector be given by Eq. (2.17). Comparing Eqs. (2.14b) and (2.17) we obtain

$$G(p) = 1 - p^2 - 2Amp^3 = \sin^2\theta\,. \tag{2.18}$$

Since Eq. (2.18) has three roots, we must identify which root we choose in order to make the mapping from the p to the θ variable unique. The three roots of Equation (2.18) for $A^2m^2 \leq \frac{1}{27}$ are given by

$$p_a = -\frac{1}{6Am}\left[2\cos\left(\frac{\Theta(\theta)}{3} + \frac{2\pi}{3}\right) + 1\right], \tag{2.19a}$$

$$p_b = -\frac{1}{6Am}\left[2\cos\left(\frac{\Theta(\theta)}{3} + \frac{4\pi}{3}\right) + 1\right], \tag{2.19b}$$

$$p_c = -\frac{1}{6Am}\left(2\cos\frac{\Theta(\theta)}{3} + 1\right), \tag{2.19c}$$

where

$$\cos\Theta(\theta) = 1 - 54A^2m^2\cos^2\theta\,. \tag{2.20}$$

At $\theta = 0$ and π, p_a in Eq. (2.19a) becomes equal to p_π given by Eq. (2.3a) and at $\theta = \pi/2$, p_a and p_b

both become equal to zero, while at $\theta = 0$ and π, p_b in Eq. (2.19b) becomes equal to p_0 given by Eq. (2.3b). Therefore, comparing with Fig. 1(a), as one increases θ from 0 to $\pi/2$ the value of p as given by Eq. (2.19b) varies from p_0 to 0, and as θ increases from $\pi/2$ to π the value of p as given by Eq. (2.19a) varies from 0 to p_π. Therefore the correct mapping from the p to the θ variable is given by

$$p = \begin{cases} -\frac{1}{6Am}\left[2\cos\left(\frac{\Theta(\theta)}{3}+\frac{4\pi}{3}\right)+1\right] & \text{for } 0 \le \theta \le \pi/2 \\ -\frac{1}{6Am}\left[2\cos\left(\frac{\Theta(\theta)}{3}+\frac{2\pi}{3}\right)+1\right] & \text{for } \pi/2 \le \theta \le \pi\,. \end{cases} \tag{2.21}$$

The null coordinates in Eq. (2.9) can be replaced by Schwarzschild-type coordinates by using (2.8) and (2.15) along with

$$t \to At\,, \tag{2.22}$$

in which case we will have

$$ds^2 = Hdt^2 - \frac{1}{H}dr^2 - \frac{2Ar^2}{H}drdp - r^2\left(\frac{1}{F}+\frac{1}{G}\right)dp^2 - r^2G(p)d\varphi^2\,, \tag{2.23}$$

where H is given by (2.10). The spherical polar angle θ is related to the p coordinate by Eq. (2.21). In the limit that $A \to 0$, the line element in Eq. (2.23) reduces to the usual Schwarzschild line element with spherical coordinates (r, θ, φ).

In the limit that $m \to 0$ the space becomes Euclidean and (2.23) and (2.10) reduce to

$$ds^2 = H_0dt^2 - \frac{1}{H_0}dr^2 - \frac{2Ar^2\sin\theta}{H_0}drd\theta - r^2\frac{1+2Ar\cos\theta}{H_0}d\theta^2 - r^2\sin^2\theta d\varphi^2\,, \tag{2.24}$$

$$H_0 = 1 + 2Ar\cos\theta - A^2r^2\sin^2\theta\,. \tag{2.25}$$

This is a special form of the flat-space line element written in a uniformly accelerating frame. Performing the coordinate transformation

$$\bar{t} = \frac{H_0^{1/2}}{A}\sinh At\,, \tag{2.26a}$$

$$\bar{\mathfrak{z}} = \frac{1}{A}(H_0^{1/2}\cosh At - 1)\,, \tag{2.26b}$$

$$\bar{\rho} = r\sin\theta\,, \tag{2.26c}$$

$$\bar{\varphi} = \varphi\,, \tag{2.26d}$$

whose inverse transformation is

$$t = \frac{1}{2A}\ln\frac{1+A(\bar{t}+\bar{\mathfrak{z}})}{1-A(\bar{t}-\bar{\mathfrak{z}})}\,, \tag{2.27a}$$

$$r^2 = \bar{\rho}^2 + \bar{z}^2\,, \tag{2.27b}$$

$$\cot\theta = \bar{z}/\bar{\rho}\,, \tag{2.27c}$$

$$\varphi = \bar{\varphi}\,, \tag{2.27d}$$

where

$$\bar{z} = \bar{\mathfrak{z}} - \tfrac{1}{2}A\bar{t}^2 + \tfrac{1}{2}A(\bar{\mathfrak{z}}^2 + \bar{\rho}^2)\,, \tag{2.28}$$

the line element (2.24) reduces to

$$ds^2 = d\bar{t}^2 - d\bar{\rho}^2 - d\bar{\mathfrak{z}}^2 - \bar{\rho}^2d\bar{\varphi}^2\,. \tag{2.29}$$

The metric in Eq. (2.29) is the usual flat-space line element written in the familiar nonaccelerating cylindrical coordinate system.

The origin of the coordinates in a coordinate system defined by the line element in Eq. (2.24) is mapped by Eqs. (2.26) onto a timelike trajectory as expressed by the inertial coordinates given by Eq. (2.29). This timelike trajectory of the point $r = 0$ is given by

$$\left(\bar{\mathfrak{z}} + \frac{1}{A}\right)^2 - \bar{t}^2 = \frac{1}{A^2} \tag{2.30}$$

and represents a uniformly accelerating motion along the $+\bar{\mathfrak{z}}$ axis of the inertial cylindrical coordinate system.

From the above arguments one can conclude that the line element in Eq. (2.23) represents a uniformly accelerating Schwarzschild-type particle accelerating along the positive $\mathfrak{z}$ axis. The coordinates (t, r, p, φ) defined by Eq. (2.23) is a coordinate system "rigidly" fixed on the accelerating particle. The center of the particle manifests its presence by a real singularity in the curvature scalar at $r = 0$. The accelerating coordinate system (t, r, p, φ) is particularly useful because the line element given by (2.23) is static and r represents the radial coordinate which is centered on the center of the particle.

The radial coordinate r in Eq. (2.23) is related to p and q coordinates by Eq. (2.8a). Therefore, the range of r is governed by the ranges of p and q given by Eqs. (2.3) and (2.21) where in (2.21) the polar angle θ is confined to the range 0 to π. Substituting (2.5) and (2.21) in (2.8a) we see that the radial coordinate r is confined to the region $r_R \ge r \ge r_S$ where

$$r_S = \begin{cases} -\dfrac{3m}{\cos\left(\frac{\Theta(\theta)}{3}+\frac{4\pi}{3}\right)+\cos\left(\frac{\delta}{3}+\frac{2\pi}{3}\right)} & \text{for } 0 \le \theta \le \frac{\pi}{2} \\ -\dfrac{3m}{\cos\left(\frac{\Theta(\theta)}{3}+\frac{2\pi}{3}\right)+\cos\left(\frac{\delta}{3}+\frac{2\pi}{3}\right)} & \text{for } \frac{\pi}{2} \le \theta \le \pi, \end{cases} \tag{2.31a}$$

$$r_R = \begin{cases} -\dfrac{3m}{\cos\left(\dfrac{\Theta(\theta)}{3}+\dfrac{4\pi}{3}\right)+\cos\left(\dfrac{\delta}{3}+\dfrac{4\pi}{3}\right)} & \text{for } 0\le\theta\le\dfrac{\pi}{2} \\ -\dfrac{3m}{\cos\left(\dfrac{\Theta(\theta)}{3}+\dfrac{2\pi}{3}\right)+\cos\left(\dfrac{\delta}{3}+\dfrac{4\pi}{3}\right)} & \text{for } \dfrac{\pi}{2}\le\theta\le\pi\,, \end{cases} \tag{2.31b}$$

$\Theta(\theta)$ and δ are given by (2.20) and (2.6), respectively.

Equations (2.26) are the transformation equations to the nonaccelerating cylindrical coordinates $(\bar{t},\bar{\rho},\bar{\delta},\bar{\varphi})$ which will be referred to as the nonaccelerating background coordinate system. This definition is in no way unique and for the vacuum C metric one cannot give an invariant definition for a nonaccelerating observer or coordinate system. In the Schwarzschild case a nonaccelerating observer is constructed by defining its four-velocity to be proportional to its timelike Killing vector. This corresponds to an invariant observer being at rest relative to the particle which is not accelerating. In the case of the vacuum C metric the timelike Killing vector does not represent the four-velocity of a nonaccelerating observer, although it uniquely defines the four-velocity of an observer being at rest with respect to the origin of the particle which is undergoing uniform acceleration. Therefore in the vacuum C metric a uniformly accelerating observer being at rest relative to the center of the accelerating particle can be given an invariant meaning, whereas an invariant inertial observer or coordinate system does not exist. The reverse case is true for the Schwarzschild metric in which an invariant meaning can be attached to the inertial coordinates while an invariant accelerating coordinate system cannot be defined. As an example of other nonaccelerating coordinate systems different from the coordinates $(\bar{t},\bar{\rho},\bar{\delta},\bar{\varphi})$ defined above, one can mention the coordinate system employed by Kinnersley and Walker[5] and Farhoosh and Zimmerman[8] in which the radiative behavior is explicitly manifested.

In order to understand the physical meaning of the Killing horizons in the $m\neq 0$ case, we will first consider the limiting case of $m=0$. The line element in this case is given by (2.24) which has a timelike Killing vector given by (2.13a), whose norm is given by (2.14a), with H being replaced by H_0 given by (2.25). The norm of the Killing vector in (2.13a) vanishes at the position determined from the condition

$$H_0 = 1 \pm 2Ar\cos\theta - A^2r^2\sin^2\theta = 0\,, \tag{2.32}$$

whose solutions are

$$r_R^0 = \frac{1}{A(1-\cos\theta)}\,, \tag{2.33a}$$

$$r_u^0 = -\frac{1}{A(1+\cos\theta)}\,. \tag{2.33b}$$

In this limit the range of radial coordinate r becomes $0=r_S^0\le r\le r_R^0$. The surface r_u^0 given by (2.33b), being negative, is out of the range of the coordinate system. The other surface, being the outer limit of the radial coordinate r given by (2.33a), is a parabola of revolution with $r=0$ at its focus. In analogy with the similar surface arising in the two-dimensional case of a uniformly accelerating coordinate system analyzed by Rindler,[13] this surface will be referred to as the Rindler surface.

Applying the transformation (2.27) to the Rindler surface given by (2.33a) we will obtain the Rindler surface expressed in the nonaccelerating coordinate system which is

$$\bar{\delta}+\frac{1}{A}=\bar{t}\,. \tag{2.34}$$

Equation (2.34) represents a $\bar{\delta}=$ const plane traveling in the positive $\bar{\delta}$ axis at the velocity of light. We see that the Rindler surface is just a manifestation of the light cone bound for points in the $\bar{\delta}=$ const plane moving at the speed of light.

Equation (2.34) can also be derived in another way. The timelike Killing vector (2.13a) as expressed in the nonaccelerating background coordinate systems takes the following form:

$$\bar{\xi}^{\mu}_{(t)} = (1+A\bar{\delta},\,0,\,A\bar{t},\,0)\,, \tag{2.35}$$

μ running from 0 to 3 denoting $\bar{t},\bar{\rho},\bar{\delta},\bar{\varphi}$, respectively. The Killing vector in (2.35) corresponds to an acceleration boost in the positive $\bar{\delta}$ direction. The norm of this Killing vector in the flat space is

$$\bar{\xi}^{\mu}_{(t)}\,\bar{\xi}_{(t)\mu} = (1+A\bar{\delta})^2 - A^2\bar{t}^{\,2}\,. \tag{2.36}$$

The vanishing of Eq. (2.36) gives the same surface as the one expressed in (2.34).

III. KILLING HORIZONS: GENERAL DISCUSSION

In this section we will discuss the structure of the Killing horizons, their shape, and their physical meaning in the general case where both A and m are different from zero. A Killing horizon is a null hypersurface, invariant under all isometries of the space-time, whose null generator is also a Killing vector. In particular if $\xi^{\mu}_{(t)}$ is a hypersurface-orthogonal Killing vector which commutes with all others, then the surfaces where $\xi^{\mu}_{(t)}\xi_{(t)\mu}=0$ are Killing horizons. In our case, we have just two independent com-

muting Killing vectors with components in the coordinates of Eq. (2.10) given by Eqs. (2.13a) and (2.13b). This makes the search for Killing horizons trivial, since we merely need to find the zeros of $H = \xi^{\mu}_{(t)}\xi_{(t)\mu}$ as expressed by Eq. (2.14a). Setting this norm equal to zero we get the trivial solution at $r = 0$ which is not relevant and will not be considered any further. The other solutions are determined from the condition $F(q) = 0$ whose solutions for $A^2m^2 < \frac{1}{27}$ are given by (2.5). Written in the accelerating spherical polar coordinates (t, r, θ, ϕ), two of these surfaces take the form given by (2.31). The third solution can be obtained in the same way by substitution (2.21) and (2.5c) in (2.8a) to give

$$r_u = \begin{cases} -\dfrac{3m}{\cos\left(\dfrac{\Theta(\theta)}{3} + \dfrac{4\pi}{3}\right) + \cos\dfrac{\delta}{3}} & \text{for } 0 \le \theta \le \dfrac{\pi}{2} \\ -\dfrac{3m}{\cos\left(\dfrac{\Theta(\theta)}{3} + \dfrac{2\pi}{3}\right) + \cos\dfrac{\delta}{3}} & \text{for } \dfrac{\pi}{2} \le \theta \le \pi . \end{cases} \tag{3.1}$$

The surface defined by (3.1) has $r_u < 0$ and lies outside of the physical range of the radial coordinate r and is unphysical and will not be considered any further.

The two remaining surfaces given by (2.31) define the only physically meaningful horizons. We will now give a description of these surfaces as seen in the accelerating and nonaccelerating coordinate systems. Equations (2.31) simplify in the forward ($\theta = 0$) and backward ($\theta = \pi$) directions as well as the equatorial plane ($\theta = \pi/2$) where they take the following forms:

$$\left.\begin{aligned} r_S &= \frac{\sqrt{3}m}{\sin\dfrac{\delta}{3}} \\ r_R &= \infty \end{aligned}\right\} \text{ for } \theta = 0 \text{ (forward direction)}, \tag{3.2}$$

TABLE I. Various numerical values for r_S/m are tabulated as a function of θ and for different numerical values of A^2m^2.

$54A^2m^2$ \ θ	0	0.2π	0.4π	0.5π	0.6π	0.8π	π
0.00	2.00	2.00	2.00	2.00	2.00	2.00	2.00
0.25	2.40	2.32	2.13	2.04	1.96	1.84	1.80
0.50	2.69	2.54	2.23	2.08	1.96	1.81	1.76
0.75	3.03	2.77	2.32	2.14	1.99	1.80	1.74
1.00	3.46	3.05	2.43	2.20	2.02	1.80	1.73
1.25	4.07	3.40	2.56	2.27	2.06	1.81	1.74
1.50	5.06	3.89	2.72	2.37	2.12	1.84	1.76
1.75	7.26	4.66	2.96	2.52	2.22	1.90	1.80
1.90	11.56	5.53	3.20	2.67	2.33	1.96	1.86
1.99	36.73	6.85	3.53	2.88	2.48	2.06	1.95
2.00	∞	7.59	3.71	3.00	2.57	2.12	2.00

$$\left.\begin{aligned} r_S &= \frac{6m}{1 + \cos\dfrac{\delta}{3} + \sqrt{3}\sin\dfrac{\delta}{3}} \\ r_R &= \frac{6m}{1 + \cos\dfrac{\delta}{3} - \sqrt{3}\sin\dfrac{\delta}{3}} \end{aligned}\right\} \text{ for } \theta = \frac{\pi}{2} \text{ (equatorial plane)}, \tag{3.3}$$

and

$$\left.\begin{aligned} r_S &= \frac{2m}{\cos\dfrac{\delta}{3} + \dfrac{1}{\sqrt{3}}\sin\dfrac{\delta}{3}} \\ r_R &= \frac{2m}{\cos\dfrac{\delta}{3} - \dfrac{1}{\sqrt{3}}\sin\dfrac{\delta}{3}} \end{aligned}\right\} \text{ for } \theta = \pi \text{ (backward direction)}. \tag{3.4}$$

In Tables I and II various numerical values for r_S and r_R are given as a function of θ for various

TABLE II. Various numerical values of r_R/m are tabulated as a function of θ and for different numerical values of A^2m^2.

$54A^2m^2$ \ θ	0	0.2π	0.4π	0.5π	0.6π	0.8π	π
0	∞	∞	∞	∞	∞	∞	∞
0.25	∞	66.22	19.16	13.57	10.61	7.93	7.26
0.50	∞	42.95	12.81	9.19	7.26	5.51	5.06
0.75	∞	32.26	9.93	7.21	5.75	4.41	4.07
1.00	∞	25.57	8.15	6.00	4.83	3.74	3.46
1.25	∞	20.68	6.89	5.14	4.17	3.27	3.03
1.50	∞	16.69	5.88	4.45	3.65	2.89	2.69
1.75	∞	13.03	4.99	3.85	3.20	2.57	2.40
1.90	∞	10.61	4.42	3.47	2.91	2.36	2.22
1.99	∞	8.42	3.91	3.13	2.66	2.19	2.06
2.00	∞	7.59	3.71	3.00	2.57	2.12	2.00

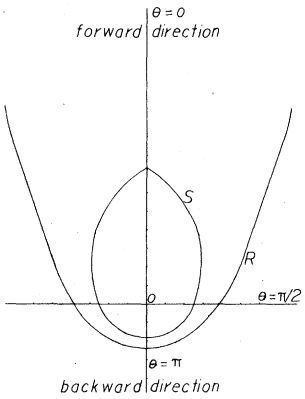

FIG. 2. The Killing horizons around a uniformly accelerating particle are plotted. The surface denoted by S is the Schwarzschild surface and the surface denoted by R is the Rindler surface which is produced by the acceleration and distorted by the mass of the particle.

values of A^2m^2, respectively. In Fig. 2 we have plotted the typical shape of these surfaces. The surface denoted by S in Fig. 2 is the Schwarzschild-type surface and from now on will be called the Schwarzschild surface. The surface denoted by R is the Rindler-type surface and will be referred to as the Rindler surface. It can be seen that the Rindler surface surrounds the Schwarzschild surface and is open in the forward direction.

The shape and the behavior of these Killing horizons will become much more apparent if the two extreme limits of very small and relatively large Am are considered. In the limit of small Am Eqs. (2.31) reduce to

$$r_S \simeq 2m(1+2Am\cos\theta)\,, \tag{3.5a}$$

$$r_R \simeq \frac{1}{A(1-\cos\theta+Am\sin^2\theta)}\,. \tag{3.5b}$$

The surface r_S given by (3.5a) is shown in Fig. 3. This surface is basically the Schwarzschild surface which is contracted in the backward direction and elongated in the forward direction. According

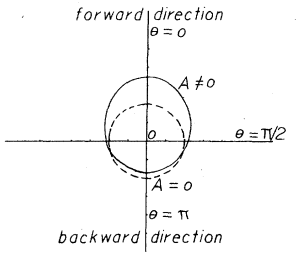

FIG. 3. This figure shows the Schwarzschild surface for a uniformly accelerating particle (the solid line) in comparison to the spherically symmetric surface for the case where $A=0$ (the dashed line).

to the approximate equation (3.5a) the larger the acceleration the more significant the deformation. The qualitative behavior of this surface is what is expected based on the principle of equivalence. The qualitative behavior of the surface can be predicted by noting that for no acceleration the Schwarzschild surface is defined as that surface where the gravitational potential of a test particle of mass μ is $\frac{1}{2}$ the rest energy or

$$\tfrac{1}{2}\mu = \frac{\mu m}{r}\,. \tag{3.6}$$

For a particle in an accelerating frame having the acceleration $\vec{A}$, the Newtonian force is modified by the principle of equivalence giving

$$\frac{\vec{F}}{\mu} = \frac{\vec{\nabla}\Phi}{\mu} + \vec{A}\,. \tag{3.7}$$

In the forward and backward directions this modifies the Newtonian potential to give

$$\Phi = \frac{\mu m}{r} \pm A\mu r\,. \tag{3.8}$$

Equating this with $\frac{1}{2}$ of the rest energy we will get an equation for the Schwarzschild surface of the form

$$r_S = \pm\frac{1}{4A}\left[1-(1\mp 16Am)^{1/2}\right], \tag{3.9}$$

where the + and − signs refer to the forward and backward directions, respectively. In the limit of small acceleration (3.9) reduces to

$$r_S \simeq 2m(1\pm 4Am)\,. \tag{3.10}$$

The qualitative behavior of Eq. (3.10) is the same as (3.5a). As the acceleration increases the Schwarzschild surface in the backward direction shrinks and in the forward direction it expands. The factor of 2 difference in these two equations often occurs when constructing the Newtonian analogy with general relativity and is not important.

The Schwarzschild surface in the form given in Eq. (3.9) has a maximum in the backward direction at $A=0$ with no minimum. On the other hand, the Schwarzschild surface in the form given in Eq. (3.4) has a minimum at $A=1/\sqrt{54}m$, i.e., according to Eq. (3.4) the Schwarzschild surface reaches its minimum distance of $r=\sqrt{3}m$ from the origin in the backward direction when the acceleration is increased to $A=1/\sqrt{54}m$. As the acceleration increases beyond $A=1/\sqrt{54}m$ this surface reverses its direction of motion in the backward direction and it expands outward. This behavior, which can also be seen in Table I, appears to violate the qualitative behavior of the principle of equivalence discussed above. The

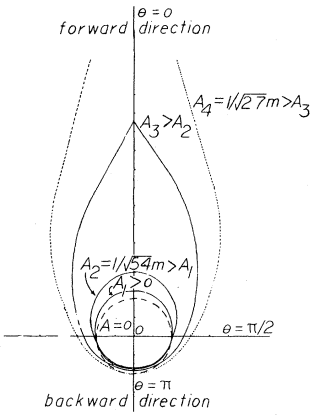

FIG. 4. In this figure we have shown the behavior of the Schwarzschild surface under the change of the acceleration. In the backward direction the surface first moves inward as the acceleration increases. At $A = 1/\sqrt{54}\,m$ it reaches its minimum distance from the origin at $r = \sqrt{3}\,m$. As the acceleration further increases the surface in the backward direction moves back outward again. In the forward direction the surface continuously expands outward as the acceleration increases. The dashed line shows the spherically symmetric Schwarzschild surface in the case of $A = 0$ and the dotted line shows the extreme limit of this surface for $A = 1/\sqrt{27}\,m$.

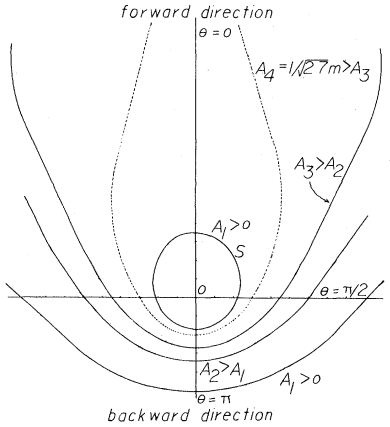

FIG. 5. The behavior of the Rindler surface under the change of the acceleration is illustrated. As the acceleration increases this surface moves inward and when A is increased to its maximum value of $A = 1/\sqrt{27}\,m$ this surface coincides with the Schwarzschild surface. The dotted line shows the extreme limit of this surface. For the sake of comparison a Schwarzschild surface for $A < 1/\sqrt{27}\,m$ is also illustrated which is denoted by S.

behavior of the Schwarzschild surface as predicted by Eq. (2.31a) and Table I is shown in Fig. 4.

As the acceleration increases the Rindler surface moves inward and finally coincides with the Schwarzschild surface that was moving outward (cf. Fig. 5). These two surfaces coincide when $A = 1/\sqrt{27}m$. In this extreme limit (2.31) reduces to

$$r_S = r_R = \begin{cases} \dfrac{6m}{1 - 2\cos\left(\dfrac{\Theta_x(\theta)}{3} + \dfrac{4\pi}{3}\right)} & \text{for } 0 \le \theta \le \dfrac{\pi}{2} \\ \dfrac{6m}{1 - 2\cos\left(\dfrac{\Theta_x(\theta)}{3} + \dfrac{2\pi}{3}\right)} & \text{for } \dfrac{\pi}{2} \le \theta \le \pi\,, \end{cases} \tag{3.11}$$

where

$$\cos\Theta_x(\theta) = 1 - 2\cos^2\theta\,. \tag{3.12}$$

The surface in Eq. (3.11) is the surface shown by the dotted line in Figs. 4 and 5. It can be seen that this surface is open in the forward direction and its distance from the origin in the backward direction is $r_S = r_R = 2m$, while in the equatorial plane it is $r_S = r_R = 3m$. As the acceleration increases just beyond the extreme value $A = 1/\sqrt{27}m$, both the Schwarzschild and Rindler surfaces become unphysical and we will have a naked singularity at the origin.

Let us now see what these surfaces appear like in a nonaccelerating coordinate system. Performing the coordinate transformation (2.27) on (2.31a), the Schwarzschild surface in a nonaccelerating frame assumes the following form:

$$[(\bar{\rho}^2 + \bar{z}^2)^{1/2}]_S = \begin{cases} -\dfrac{3m}{\cos\left(\dfrac{\bar{\Theta}}{3} + \dfrac{4\pi}{3}\right) + \cos\left(\dfrac{\bar{\delta}}{3} + \dfrac{2\pi}{3}\right)} & \text{for } 0 \le \bar{\theta} = \arccos\dfrac{\bar{z}}{(\bar{\rho}^2 + \bar{z}^2)^{1/2}} \le \dfrac{\pi}{2} \\ -\dfrac{3m}{\cos\left(\dfrac{\bar{\Theta}}{3} + \dfrac{2\pi}{3}\right) + \cos\left(\dfrac{\bar{\delta}}{3} + \dfrac{2\pi}{3}\right)} & \text{for } \dfrac{\pi}{2} \le \bar{\theta} \le \pi\,. \end{cases} \tag{3.13}$$

In a similar manner the Rindler surface in (2.31b) becomes

$$[(\bar{\rho}^2 + \bar{z}^2)^{1/2}]_R = \begin{cases} -\dfrac{3m}{\cos\left(\dfrac{\bar{\Theta}}{3} + \dfrac{4\pi}{3}\right) + \cos\left(\dfrac{\bar{\delta}}{3} + \dfrac{4\pi}{3}\right)} & \text{for } 0 \le \bar{\theta} \le \dfrac{\pi}{2} \\ -\dfrac{3m}{\cos\left(\dfrac{\bar{\Theta}}{3} + \dfrac{2\pi}{3}\right) + \cos\left(\dfrac{\bar{\delta}}{3} + \dfrac{4\pi}{3}\right)} & \text{for } \dfrac{\pi}{2} \le \bar{\theta} \le \pi\,, \end{cases} \tag{3.14}$$

where

$$\cos\bar{\delta} = -(1 - 54A^2m^2), \tag{3.15}$$

$$\cos\bar{\Theta} = 1 - 54A^2m^2\frac{\bar{z}^2}{\bar{\rho}^2+\bar{z}^2}, \tag{3.16}$$

and $\bar{z}$ is given by (2.28). In the limit of small acceleration (3.13) and (3.14) become

$$\bar{z}_S{}^2 \equiv [\bar{\delta}_S - \tfrac{1}{2}A\bar{t}^2 + \tfrac{1}{2}A(\bar{\delta}_S{}^2 + \bar{\rho}_S{}^2)]^2$$
$$\simeq \bar{\rho}_S{}^2 - 4m^2(1+2A\bar{z}_S), \tag{3.17}$$

$$\bar{\rho}_R{}^2 \simeq \frac{1}{A^2}[1+2A(\bar{z}_R - m)]. \tag{3.18}$$

At time $\bar{t}=0$ Eqs. (3.17) and (3.18) read as

$$\bar{\rho}_S{}^2 + \bar{\delta}_S{}^2 \simeq 4m^2(1+A\bar{\delta}), \tag{3.19}$$

$$\bar{\rho}_R \simeq \frac{1}{A}[1+A(\bar{\delta} - m)]. \tag{3.20}$$

The surface S given by (3.19) is the deformed Schwarzschild surface similar to the surface r_S in the accelerating frame, while the surface R given by (3.20) is a plane which is slightly distorted due to the mass of the particle m. The time enters into the evolution of these surfaces only through the term $\bar{\delta} - \frac{1}{2}A\bar{t}^2$, which is the familiar term representing the distance traveled in the positive $\bar{\delta}$ axis due to the acceleration A in the time $\bar{t}$. Therefore as time increases the surfaces are carried along with the particle which is uniformly accelerating along the $\bar{\delta}$ axis.

IV. RADIAL GEODESICS; PRINCIPLE OF EQUIVALENCE AND THE DRAGGING OF THE INERTIAL FRAME

In this section we will investigate the behavior of the radial geodesics as seen in the rest frame of the particle. For small acceleration we will show that the behavior of the geodesics can be explained in terms of the principle of equivalence and the dragging of the inertial frame.

Let us consider the radial geodesics expressed by the coordinates in Eq. (2.23). From the constant of motion defined by the timelike Killing vector (2.13a) we can immediately obtain the four-velocity of the radial geodesics. For timelike geodesics, i.e., when the four-velocity vector v^μ satisfies the condition

$$v^\mu v_\mu = +1 \tag{4.1}$$

this radial four-velocity vector is

$$v^\mu = \left(\frac{dt}{ds}, \frac{dr}{ds}, 0, 0\right) = \left(\frac{E}{H}, \pm(E^2 - H)^{1/2}, 0, 0\right). \tag{4.2}$$

E is the constant of motion defined by the timelike Killing vector and H is defined in (2.10). From (4.2) we have

$$\dot{r}^2 = E^2 - H, \tag{4.3}$$

where the dot denotes d/ds. In this equation $\dot{r}^2$ is basically the kinetic energy of the test particle, E^2 is the total energy, and H is the potential energy.

To obtain the qualitative behavior of this path we will restrict ourselves to the simplest case of motion along the axis of symmetry. In this case the potential $V(r) \equiv H$ given by (2.10) becomes

$$V_{+(-)}(r) = 1 - \frac{2m}{r} + 6Amp_{0(\pi)} + Ar(G,p)_{0(\pi)}. \tag{4.4}$$

p_0 and p_π are given by Eqs. (2.3) and the + and − signs refer to the forward and the backward directions, respectively.

These two potentials are plotted in Fig. 6 for different values of the acceleration A. In the forward direction the plots cross the zero level of energy once and exactly at the position of the Schwarzschild surface, and due to the fact that our coordinate system is defined only outside the Schwarzschild surface we are only interested in the part of these plots which are drawn in solid face in Fig. 6(a). We saw in the previous section that as the acceleration increases the Schwarzschild surface in the forward direction expands outward. This behavior can also be seen in Fig. 6(a) where for larger accelerations the plot crosses the zero level of energy at a farther distance from the origin, until at the extreme limit of $A = 1/\sqrt{27}m$ the potential curve never crosses the zero level of energy. Furthermore, the potential energy in the forward direction has no maximum and all these radial geodesics are bounded by the potential and will collide with the particle. The reason for this is obvious. An accelerating particle will always eventually overtake any free-falling object. This will not be the case for a test particle in the backward direction. Another interesting feature of this potential is shown in

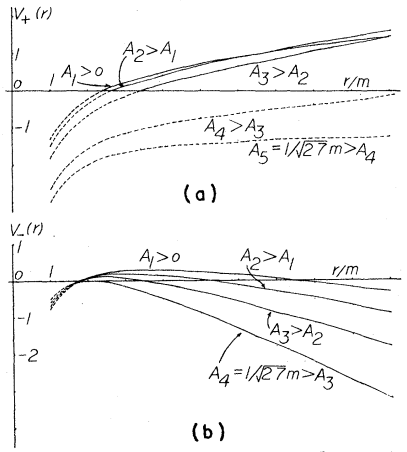

FIG. 6. This is a plot of gravitational potential of a uniformly accelerating particle for different values of acceleration in (a) the forward direction and (b) the backward direction.

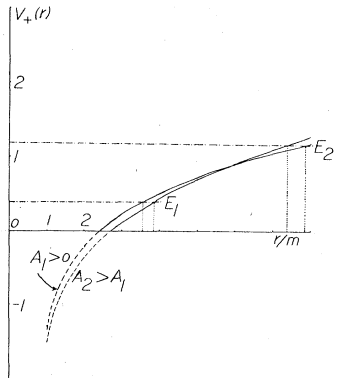

FIG. 7. This figure shows the behavior of the radial timelike geodesics in the forward direction.

Fig. 7. It can be seen in this figure that a test particle which has energy E_1 can be found further away from the origin for larger accelerations. The reverse is true for a test particle with sufficiently large energy such as E_2 in which case the larger the acceleration the smaller the maximum distance the test particle can be from the origin.

In the backward direction the potential energy curves cross the zero-energy level twice at the positions of the Schwarzschild and Rindler surfaces. In the backward direction the potential $V_-(r)$ has a maximum determined from

$$\frac{m}{r^2} = -\frac{1}{12m}\left[1 - 4\cos^2\left(\frac{\lambda}{3} + \frac{2\pi}{3}\right)\right], \tag{4.5}$$

where λ is given in Eq. (2.4). Unlike the forward direction in which all the radial geodesics are bounded by the potential and will collide with the particle, the geodesics in the backward direction may or may not fall on the accelerating particle depending on their energy. This situation is shown in Fig. 8. In this figure the geodesics having energy E_1 are not bound and they may escape. The backward geodesics having energy E_3 are trapped in a region $r \leq r_1$ or $r \geq r_2$ by the effect of the dragging of the inertial frame. Points r_1 and r_2 are the turning points of a test particle

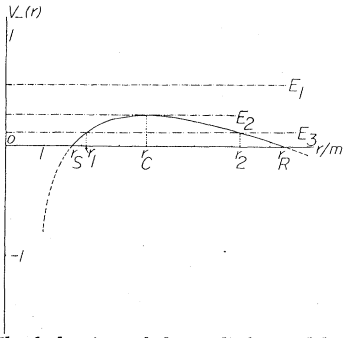

FIG. 8. The behavior of the radial timelike geodesics in the backward direction is shown in this figure.

of energy E_3. The geodesic having energy E_2 lies on an asymptotic orbit. A test particle with this energy will either asymptotically approach or recede from the position at $r = r_c$. At $r = r_c$ the test particle is static with respect to the accelerating particle.

For small acceleration the forward and the backward potentials given by (4.4) reduce to

$$V_+(r) \simeq 1 - \frac{2m}{r} - 6Am + 2Ar(1 - 2Am), \tag{4.6}$$

$$V_-(r) \simeq 1 - \frac{2m}{r} + 6Am - 2Ar(1 + 2Am). \tag{4.7}$$

In Eqs. (4.6) and (4.7) one can identify the term $\pm 2Ar$ with the principle of equivalence and the term A^2mr can be identified with the effect of the dragging of the inertial frame. In order to see this connection more clearly we notice that in the limit of small acceleration Eq. (4.5) can be written as

$$\frac{m}{r^2} \simeq A(1 + 2Am). \tag{4.8}$$

Equation (4.8) gives the approximate position of the static observer discussed in the previous paragraph. The term m/r^2 on the left-hand side of this equation is the Newtonian gravitational acceleration which to lowest order in A equals the acceleration of the particle. This is just what would have been expected from the principle of equivalence discussed in Sec. III. The second term on the right-hand side of Eq. (4.8), i.e., $2A^2m$, has no classical analog and represents the effect of the dragging of the inertial frame produced by the rectilinear acceleration.

V. RADIAL TIMELIKE TRAJECTORIES

In this section we will discuss the motion along an arbitrary radial timelike trajectory. The four-velocity vector of any radial path expressed in the accelerating coordinates (t, r, p, φ) is given by

$$v^\mu = \left(\frac{dt}{ds}, \frac{dr}{ds}, 0, 0\right) \equiv \gamma(1, v, 0, 0), \tag{5.1}$$

where

$$\gamma \equiv \frac{dt}{ds}, \tag{5.2a}$$

$$v \equiv \frac{dr}{dt}. \tag{5.2b}$$

For a timelike path one must have

$$v^\mu v_\mu = +1. \tag{5.3}$$

Using the line element (2.23), Eq. (5.3) gives us an expression for γ:

$$\gamma = \pm \frac{\sqrt{H}}{(H^2 - v^2)^{1/2}}, \tag{5.4}$$

where H is given by (2.10). Substituting (5.4) back in (5.1) one has

$$v^{\mu} = \pm \left(\frac{H}{H^2 - v^2}\right)^{1/2} (1, v, 0, 0) . \tag{5.5}$$

Radial timelike trajectories do not exist for all values of r. The denominator of equation (5.5) is real only if

$$H^2 - v^2 > 0 . \tag{5.6}$$

The radial velocity v is the velocity as expressed in the accelerating coordinates. This velocity is bounded by

$$-H \leq v \leq H . \tag{5.7}$$

In general the radial velocity can assume any value in the range ($-H$ to $+H$). On the Killing horizons the function H changes sign and the radial paths discussed above become spacelike.

In analogy with the Kerr metric, the observer which is at rest with respect to the accelerating particle will be called the "static" observer. As viewed from the nonaccelerating frame the static observer would appear to be uniformly accelerating in the positve $\hat{\imath}$ direction along with the particle.

VI. SUMMARY AND CONCLUSIONS

The Schwarzschild metric representing the gravitational field of a spherically symmetric static particle is known to have a spherically symmetric Killing horizon at $r = 2m$. Any kind of motion causes this spherically symmetric surface to become distorted. For example, the Kerr metric representing the gravitational field of a uniformly rotating particle reveals two Killing horizons. One is the Schwarzschild surface being deformed. The deformation is of the form of a contraction around the poles. The larger the rotation the more significant the deformation. The other Killing horizon is being caused mainly by the rotation and distorted by the mass of the parti cle. We saw in this paper that a uniform rectilinear acceleration has a somehwat similar effect, in the sense that a uniformly accelerating particle has two Killing horizons. One is the Schwarzschild surface being caused by the mass and distorted by the acceleration. The distortion is of the form of an expansion in the forward direction and a contraction in the backward direction. The larger the acceleration the more significant the deformation of this surface. The other Killing horizon is being produced mainly due to the acceleration and is being slightly distorted due to the mass of the particle. As seen in an accelerating frame with respect to which the accelerating particle appears to be at rest, this Rindler surface has a shape similar to a parabola or revolution being open in the forward direction and surrounds the Schwarzschild surface. The Rindler surface is just a manifestation of the light cone representing the points traveling at the speed of light.

By increasing the acceleration the Schwarzschild surface becomes more distorted. It becomes contracted in the backward direction and elongated in the forward direction. This phenomenon was anticipated from the principle of equivalence. However, when the acceleration reaches $A = 1/\sqrt{54}m$, the Schwarzschild surface reaches its maximum contraction in the backward direction and increasing the acceleration beyond this magnitude the Schwarzschild surface in the backward direction expands outward. This behavior appears to be a violation of the principle of equivalence.

When the acceleration is increased the Rindler surface moves inward. The acceleration can be increased up to $A = 1/\sqrt{27}m$ where the Rindler and the Schwarzschild surfaces coincide forming a naked singularity at the origin. As viewed by a nonaccelerating inertial observer, these surfaces appear to be carried along with the accelerating particle.

The timelike geodesics in the forward direction are bound and a timelike test particle is not allowed to go beyond a certain distance from the accelerating particle. In the backward direction the timelike geodesics may or may not be bound depending on their energy. A test particle in this direction can be dragged along with the accelerating particle and remain stationary with respect to it. This is the effect of the dragging of the inertial frame produced by the rectilinear acceleration.

ACKNOWLEDGMENT

This work was supported by the National Aeronautics and Space Administration under Grant No. NSG-7639.

[1] T. Levi-Civita, Atti Accad. Naz. Lincei Cl. Sci. Fis. Mat. Nat. Rend. 27, 343 (1918).
[2] E. Newman and L. Tamburino, J. Math. Phys. 2, 667 (1961).
[3] I. Robinson and A. Trautman, Proc. R. Soc. London A265, 463 (1962).
[4] J. Ehlers and W. Kundt, in *Gravitation, an Introduction to Current Research*, edited by L. Witten (Wiley, New York, 1962).
[5] W. Kinnersley and M. Walker, Phys. Rev. D 2, 1359 (1970).
[6] J. F. Plebanski and M. Demianski, Ann. Phys. (N. Y.) 98, 98 (1976).
[7] F. J. Ernst, J. Math. Phys. 17, 515 (1976).
[8] H. Farhoosh and R. L. Zimmerman, J. Math. Phys. 20, 2272 (1979).
[9] B. B. Godfrey, Gen. Relativ. Gravit. 3, 3 (1972).
[10] B. B. Godfrey, J. Math. Phys. 12, 606 (1971).
[11] B. Carter, Commun. Math. Phys. 10, 280 (1968).
[12] L. P. Hughston, Commun. Math. Phys. 32, 147 (1973).
[13] W. Rindler, Am. J. Phys. 34, 1174 (1966).
[14] For a discussion of cubic equations see, for example, D. S. Meyler and O. G. Sutton in *A Compendium of Mathematics and Physics* (The English Universities Press, London, 1958).